



Comparative polypharmacokinetics of nine anti-inflammatory components of Jinyinhua (*Lonicerae Japonicae Flos*) and Shanyinhua (*Lonicerae Flos*) in mice with p-xylene-induced ear edema

LI Haiying^{a, b†}, XIAO Meifeng^{a, b, c†}, PAN Xue^{a, b, c}, LI Wenjiao^{a, b}, ZHOU Yiqun^{a, b, c}, LIU Wenlong^{a, b, c}, HE Fuyuan^{a, b, c*}

a. College of Pharmacy, Hunan University of Chinese Medicine, Changsha, Hunan 410208, China

b. Hunan Key Laboratory of Druggability and Preparation Modification for Traditional Chinese Medicine, Changsha, Hunan 410208, China

c. Supramolecular Mechanism and Mathematic-Physics Characterization for Chinese Materia Medica, Hunan University of Chinese Medicine, Changsha, Hunan 410208, China

ARTICLE INFO

Article history

Received 08 November 2022

Accepted 26 January 2023

Available online 25 March 2023

Keywords

Jinyinhua (*Lonicerae Japonicae Flos*, LJF)

Shanyinhua (*Lonicerae Flos*, LF)

Polypharmacokinetics (PPK) model

Total quantum statistical moment similarity (TQSMS) method

Anti-inflammatory efficacy

Consistency

ABSTRACT

Objective To reveal the integral *in vivo* polypharmacokinetics (PPK) similarity or difference between Jinyinhua (*Lonicerae Japonicae Flos*, LJF) and Shanyinhua (*Lonicerae Flos*, LF), and provide reference for their clinical application.

Methods The PPK model and its total quantum statistical moment similarity (TQSMS) method were used to compare the integral PPK profiles of nine components with anti-inflammatory efficacy (rutin, caffeic acid, chlorogenic acid, cryptochlorogenic acid, dispsacoside B, macranthoidin B, isochlorogenic acid A, isochlorogenic acid B, and isochlorogenic acid C) of LJF and LF. A total of 54 Specific Pathogen Free (SPF) grade Kunming (KM) mice were randomized into LJF group and LF group ($n = 27$), and each group was divided into nine subgroups ($n = 3$) according to different time points. Subsequently, mice model of p-xylene-induced ear edema was constructed by oral administration of LJF and LF. The concentrations of the nine anti-inflammatory components in plasma samples of the mice were determined by ultra-performance liquid chromatography/quadrupole time-of-flight mass spectrometry (UP-LC-QTOF-MS/MS). And the pharmacokinetics (PK) parameters of single component and the integral PPK parameters [total quantum statistical moment (TQSM) and TQSMS] of multiple components were calculated by Drug And Statistics (DAS) software and home-brew programs with Excel, respectively.

Results There were significant differences in single-component PK parameters between LJF and LF ($P < 0.05$). Whereas, no significant differences were found in multi-component TQSM parameters, including total quantum zero moment (AUC_{T0-t} , $AUC_{T0-\infty}$) and total quantum first moment (MRT_{T0-t} , $MRT_{T0-\infty}$) for the total quanta ($P > 0.05$). Accordingly, single-component TQSMS varied from 0.220 4 to 0.968 9, and that for the total quanta was 0.828 4, suggesting no significant differences in the speed and extent of bioavailability between LJF and LF. Furthermore, in light of high TQSMS (0.828 4), the integral PPK profiles of the nine anti-inflammatory components of LJF and LF were similar under 90% confidence intervals.

Conclusion The PPK model and its TQSMS method are appropriate and efficient to compare

†These authors contributed equally.

*Corresponding author: HE Fuyuan, E-mail: pharmsharking@163.com.

Peer review under the responsibility of Hunan University of Chinese Medicine.

DOI: [10.1016/j.dcmcd.2023.02.009](https://doi.org/10.1016/j.dcmcd.2023.02.009)

Citation: LI HY, XIAO MF, PAN X, et al. Comparative polypharmacokinetics of nine anti-inflammatory components of Jinyinhua (*Lonicerae Japonicae Flos*) and Shanyinhua (*Lonicerae Flos*) in mice with p-xylene-induced ear edema. *Digital Chinese Medicine*, 2023, 6(1): 73-85.

the similarity or difference of integral PPK profiles of multi-component herbal medicines. It is suggested in this research that LJF can be replaced with LF or vice versa for anti-inflammatory treatment.

1 Introduction

Jinyinhua (*Lonicerae Japonicae Flos*, LJF) is dry flower buds or new blossom of *Lonicera japonica* Thunb., mainly grown in China, Japan, and Korea. Shanyinhua (*Lonicerae Flos*, LF), primarily found in China, is also dry buds or new blossom of *Lonicera macranthoides* Hand.-Mazz., *Lonicera hypoglauca* Miq., *Lonicera confusa* DC., or *Lonicera fulvotomentosa* Hsu et S. C. Cheng [1]. Both LJF and LF are capable of clearing heat and toxins, and evacuating wind heat with anti-inflammatory, antiviral, antidiabetic, antiallergic, and antioxidant effects [2]. According to the *Chinese Pharmacopoeia* (editions 1977, 1985, 1990, 1995, and 2000), LJF can also be originated from *Lonicera hypoglauca* Miq., *Lonicera confuse* DC., and *Lonicera dasystyla* Rehd., i.e. the three plant sources of LF we introduced above. Both LJF and LF had been indiscriminately used as the same Chinese material medica (CMM) until the *Chinese Pharmacopoeia* (edition 2005) came out, which lists LF and LJF as two separate CMMs due to their different component concentrations [3]. For instance, LF contains more organic acids and saponins than LJF does, while LJF contains more flavonoids than LF [3]. Although LJF differs from LF in the component concentration, they have same clinical efficacy in accordance with the *Chinese Pharmacopoeia* (editions 2005, 2010, 2015, and 2020). On account of the controversy over their separate listing, and inconsistency between components *in vitro* and their therapeutic efficacy, disagreements on the clinical applications of LJF and LF have risen and continued until now. Essentially, the controversy lies in the enormous differences in the component concentration *in vitro* but the great similarities in therapeutic efficacy [4-6]. Therefore, it is necessary to investigate the two CMMs' *in vivo* bioavailability to help explain the inconsistency between components *in vitro* and their therapeutic efficacy.

To date, there is numerous literature regarding the chemical composition and pharmacological efficacy of LJF and LF. And the pharmacokinetics (PK) profiles of several important parameters of components in LJF and its compound prescriptions had been investigated [7, 8]. However, there are few comparative studies on polypharmacokinetics (PPK) between LJF and LF. PK plays an essential role in evaluating CMM's bioavailability, providing references to the therapeutic efficacy and safety of a single component in CMM [9, 10]. However, it would be time-consuming and labor-intensive when the PK model is applied for assessing numerous components in the

CMM. In particular, single-component PK parameters vary dramatically due to the wide concentration range of the components and their complex interactions *in vivo*, thus challenging in technologies [11, 12]. Furthermore, CMM has synergetic effects derived from the integration of multiple components. Therefore, it is imperative to assess the similarity or difference of integral PPK profiles of multiple components using PPK model.

PPK model plays an important role in comparing the bioavailability and clinical efficacy of multi-component CMMs, thereby providing evidence for the CMMs' clinical application and for analyzing their clinical efficacy with their different sources. The components and their concentrations of CMMs are often complex and changeable, but their pharmacological efficacy may be similar, which is difficult to explain with previous methods. Therefore, HE et al. [13] constructed a PPK model and its total quantum statistical moment similarity (TQSMS) method based on statistical moment theory (SMT) to integrate single-component statistical moment (SM) parameters to constitute total quantum statistical moment (TQSM) parameters and TQSMS for better analyzing the difference and similarity of multiple components of CMMs by recording the time course of plasma concentrations (location, mean residence time, and variance of the residence time). The PPK model has been managed to screen quality-marker from numerous components in Buyang Huanwu Injection (补阳还五注射剂) based on TQSMS [14]. Moreover, the PPK model was also employed to evaluate the interactions between midazolam and flucloxacillin [15]. In addition, TQSMS method could be applied to evaluate the similarity of two chromatographic fingerprints [16]. In this study, the PPK profiles of LJF and LF were compared with the use of PPK model built beforehand.

It is reported that the anti-inflammatory effects and mechanisms of LJF and LF are similar [5]. Consequently, components with anti-inflammatory efficacy, nine in total, were selected for research [17-20]. Mice with P-xylene-induced ear edema are typical research models with inflammations. They are easy to breed, economical, and highly reproductive. In this research, the similarity or difference of the integral PPK profiles of the nine anti-inflammatory components of LJF and LF in mice with p-xylene-induced ear edema were investigated by comparison of their PPK profiles and its TQSMS, laying a foundation for explaining the inconsistency between *in vitro* components and the clinical effects of LJF and LF, and providing references for their clinical application.

2 Materials and methods

2.1 PPK model and its TQSMS method

2.1.1 PPK model For single component PK profiles, the typical SM parameters as zero moment, first moment, and second moment could be obtained by methods from literature [21, 22]. A holistic PPK profile (HPP) was constituted of n kinds of PK profiles, which should be defined to the integral PPK profile as total quantum zero moment (AUC_T), total quantum first moment (MRT_T), and total quantum second moment (VRT_T) as the following.

AUC_T for a HPP, which is defined as the area under concentration-time curve, can be expressed by Equation (1). AUC_{0-t} and $AUC_{0-\infty}$ represent the area under concentration-time curve from time 0 to t and time 0 to infinite, respectively.

$$AUC_T = \sum_{i=1}^n AUC_i \tag{1}$$

MRT_T for a HPP, representing the residence time on average, is composed of n kinds of individual PK profiles, and can be given as Equation (2). MRT_{0-t} and $MRT_{0-\infty}$ represent the residence time on average from time 0 to t and time 0 to infinite, respectively.

$$MRT_T = \sum_{i=1}^n MRT_i \cdot AUC_i / \sum_{i=1}^n AUC_i \tag{2}$$

VRT_T for a HPP is defined as the variance of MRT_T and can be used to describe the dispersion degree of these single-component PK profiles, expressed in Equation (3). $VRT_{0-\infty}$ represents the variance of MRT_T from time 0 to infinite.

$$VRT_T = \sum_{i=1}^n [(MRT_i^2 VRT_i) \cdot AUC_i] / \sum_{i=1}^n AUC_i - MRT_T^2 \tag{3}$$

2.1.2 TQSMS method The two TQSM parameters, MRT_T and VRT_T , on behalf of center or dispersion of residence time respectively, can be converted into normal distribution probability density function (NDPDF), shown as the following Equation (4).

$$F(t) = \int_{-\infty}^{\infty} [1/\sqrt{2\pi} \cdot \sigma] \cdot \exp[-(t-\bar{t})^2/2\sigma^2] dt \tag{4}$$

$(-\infty < t < +\infty)$

t , \bar{t} , and σ^2 stand for PK time, MRT_T , and VRT_T , respectively. Assuming that the first moments of two PK profiles were \bar{t}_a , \bar{t}_b , and the second moments were σ_a^2 , σ_b^2 respectively, and the cross points of two normal distribution curves could be represented with t_1 and t_2 .

The TQSMS of the two PPK curves can be defined as the overlapped area for two NDPDFs surrounding with

t -axis depicted as Equation (5). Figure 1 shows the PPK model and the TQSMS method.

$$S_T = 1 - \left| \int_{t_1}^{t_2} [1/\sqrt{2\pi} \cdot \sigma_a] \cdot \exp[-(t-\bar{t}_a)^2/2\sigma_a^2] dt - \int_{t_1}^{t_2} [1/\sqrt{2\pi} \cdot \sigma_b] \cdot \exp[-(t-\bar{t}_b)^2/2\sigma_b^2] dt \right| \tag{5}$$

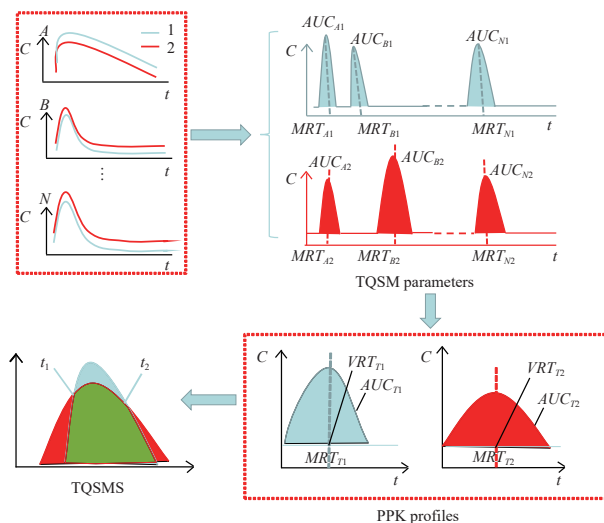


Figure 1 PPK model and the TQSMS method for multiple components

c represents concentration. t represents time. A, B, and N represent different components, respectively. 1 and 2 represent CMM1 and CMM2, respectively. AUC_{A1} and MRT_{A1} represent the AUC and MRT of component A in CMM1, respectively. AUC_{B1} and MRT_{B1} represent the AUC and MRT of component B in CMM1, respectively. AUC_{N1} and MRT_{N1} represent the AUC and MRT of component N in CMM1, respectively. Accordingly, AUC_{A2} and MRT_{A2} , AUC_{B2} and MRT_{B2} , AUC_{N2} and MRT_{N2} for CMM2 are the same as CMM1. AUC_{T1} , MRT_{T1} , and VRT_{T1} represent the total quanta of all the N components in CMM1. Likely, AUC_{T2} , MRT_{T2} , and VRT_{T2} represent the total quanta of all the N components in CMM2.

2.2 Chemicals and reagents

LJF and LF were purchased from Hunan Zhenxing Traditional Chinese Medicine Co., Ltd. (China) and authenticated as dry flower buds of *Lonicera japonica* Thunb. and that of *Lonicera macranthoides* Hand.-Mazz., respectively by Professor ZHOU Xiaojiang (Hunan Provincial Research Center for Standardization and Functional Engineering Technology of Decoction Pieces of Traditional Chinese Medicine, China). Chlorogenic acid (purity = 96.8%) was purchased from the National Institute for the Control of Pharmaceutical and Biological Products (China). Rutin (purity \geq 98%), caffeic acid (purity \geq 98%), cryptochlorogenic acid (purity \geq 98%), isochlorogenic acid A (purity \geq 98%), isochlorogenic acid B (purity \geq 98%), isochlorogenic acid C (purity \geq 98%), dipscoside B (purity \geq 98%), and macranthoidin B (purity \geq 98%) were purchased from Shanghai Yuanye

Bio-Technology Co., Ltd. (China). **Figure 2** shows the chemical structures of all the above nine anti-inflammatory components in LJF and LF. Acetonitrile and methanol of high-performance liquid chromatograph (HPLC) grade were obtained from Merck Co., Ltd. (Germany). P-xylene of analytical grade was purchased from Shanghai Wokai Biotechnology Co., Ltd. (China). All other chemical reagents employed in the experiments were of analytical grade.

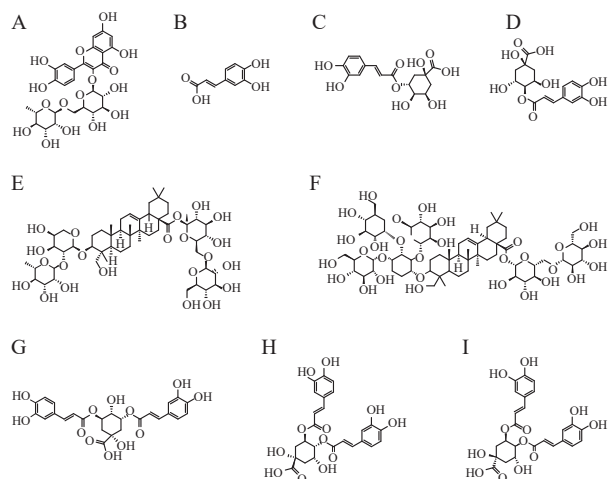


Figure 2 Chemical structures of the nine anti-inflammatory components in LJF and LF

A, rutin. B, caffeic acid. C, chlorogenic acid. D, cryptochlorogenic acid. E, dipsacoside B. F, macranthoidin B. G, isochlorogenic acid A. H, isochlorogenic acid B. I, isochlorogenic acid C.

2.3 Experimental apparatus and conditions

For ultra-performance liquid chromatography/quadrupole time-of-flight mass spectrometry (UPLC-QTOF-MS/MS) analysis, an Agilent 1290 UPLC system was coupled to the 6530 Quadrupole Time-of-Flight Mass Spectrometer (Agilent Company, USA) equipped with

electronic spray ionization (ESI) source. The chromatographic separation was performed on a Waters ACQUITY MPLC BEH Sniel RP18 Column (1.7 μm , 2.1 mm \times 50 mm) at 30 $^{\circ}\text{C}$. A mixture of solvent A (acetonitrile) and solvent B (0.1% formic acid solution) was used as the mobile phase at a flow rate of 0.3 mL/min. The gradient elution procedures were: 0 – 10 min, 5% – 20% A; 10 – 15 min, 20% – 35% A; 15 – 25 min, 35% – 83% A. Then, 3 μL of assayed samples was injected into the apparatus. Mass spectrometry were set as follows: ESI temperature, 400 $^{\circ}\text{C}$; ion transfer tube temperature, 250 $^{\circ}\text{C}$; interface temperature, 300 $^{\circ}\text{C}$; atomizing gas flow rate, 2.7 L/min; heating gas flow rate, 10 L/min; mass spectrometry voltage, 5 500 V. ESI in negative mode was applied for processing the nine components, using multiple reaction monitoring (MRM) with the precursor/production pairs. The component concentration of assayed samples were analyzed with Mass Hunter quantitative analysis software (V.5.0, Agilent). **Table 1** lists the summary of component information and the corresponding MRM parameters of the nine anti-inflammatory components in LJF and LF.

2.4 Preparation of LJF and LF extraction solutions

Water extraction method was adopted to prepare the LJF and LF extraction solutions according to the chemical structures and properties of the above nine components. LJF of 100 g was extracted by refluxing with water (1 : 12, w/v) for 45 min, and followed by filtration. Subsequently, the filter residue was extracted again with 10-fold the amount of water used previously. Then, the above two filtrates were merged and evaporated by rotary evaporation and concentrated to 90 mL (crude drug concentration was 1.11 g/mL). LF extraction solution was obtained using the same method. The two solutions were kept at 4 $^{\circ}\text{C}$ for further research.

Table 1 Component information and corresponding MRM parameters of the nine anti-inflammatory components in LJF and LF

No.	Component	Retention time (min)	Molecular formula	Molecular weight	Precursor/Production ion (m/z)	Collision energy (eV)
1	Rutin	11.79	$\text{C}_{27}\text{H}_{30}\text{O}_{16}$	610.107 3	609.1/300.0	– 30
2	Caffeic acid	6.98	$\text{C}_9\text{H}_8\text{O}_4$	180.150 0	179.0/135.0	– 20
3	Chlorogenic acid	6.33	$\text{C}_{16}\text{H}_{18}\text{O}_9$	354.169 2	353.1/191.0	– 20
4	Cryptochlorogenic acid	5.90	$\text{C}_{16}\text{H}_{18}\text{O}_9$	354.088 1	353.1/173.0	– 20
5	Dipsacoside B	15.62	$\text{C}_{53}\text{H}_{86}\text{O}_{22}$	1 090.104 0	1 073.6/749.4	– 45
6	Macranthoidin B	15.03	$\text{C}_{65}\text{H}_{106}\text{O}_{32}$	1 398.894 5	1 397.7/1 073.3	– 45
7	Isochlorogenic acid A	13.28	$\text{C}_{25}\text{H}_{24}\text{O}_{12}$	516.147 7	515.1/353.0	– 22
8	Isochlorogenic acid B	12.84	$\text{C}_{25}\text{H}_{24}\text{O}_{12}$	516.146 2	515.1/353.0	– 26
9	Isochlorogenic acid C	13.90	$\text{C}_{25}\text{H}_{24}\text{O}_{12}$	516.150 8	515.1/353.0	– 24

2.5 Pharmacokinetic study

Specific Pathogen Free (SPF) male grade Kunming (KM) mice (22 – 25 g) were purchased from Hunan Slack Jingda Experimental Animal Co., Ltd. [SCXK (Xiang) 2019-0004]. All mice were kept in a SPF grade experimental animal center [SYXK (Xiang) 2019-0009]. The mice were housed in a controlled environment (temperature at 22 °C, relative humidity of 50%, and 12/12 h dark-light cycle) with free access to food and water for one week. All animal experiments were conducted in accordance with the guidelines of the Animal Experimental Ethics Committee of the Hunan University of Chinese Medicine (LL2019092509).

A total of 54 KM mice were randomly assigned to two groups ($n = 27$) [each group was divided into nine subgroups ($n = 3$) according to different time points], and labeled as LJF group and LF group. All mice had free access to water for 12 h before experiment. The ear edema of mice were induced by applying 25 μ L of p-xylene to the front and back sides of the left ear 0.5 h after administration of LJF or LF in accordance with procedures reported previously [19]. Significant signs of ear edema proved the successful establishment of the models. Mice were orally administered LJF extraction solution or LF extraction solution at a dose of 30 g/kg body weight, respectively. And blood samples were collected at 0.08, 0.25, 0.50, 0.75, 1.00, 2.00, 4.00, 6.00, and 8.00 h after single-dose administration. Samples were stored in heparin sodium anti-coagulation tubes, and then processed by centrifugation at 4 000 r/min for 15 min within 1 h to get the plasma.

2.6 Sample preparation

First, 4% phosphoric acid solution was obtained by diluting 4.7 mL of 85% phosphoric acid with water to 100 mL. And 2 mL of mice plasma supernatant was thoroughly mixed with 2 mL of 4% phosphoric acid solution for centrifugation at 12 000 r/min. Then, the supernatant was placed on the OASIS HLB solid phase extraction cartridge, which was washed with 2 mL of 5% methanol, then with 2-fold the amount of methanol to elude the test substance. The methanol solution was collected and blown dry with nitrogen stream. The residue was dissolved in 200 μ L methanol and centrifuged as described above. Afterwards, the supernatant was taken into a sample vial for test.

2.7 Preparation of calibration standards and quality control (QC) samples

Individual stock solutions of rutin, caffeic acid, chlorogenic acid, cryptochlorogenic acid, dispsacoside B, macranthoidin B, isochlorogenic acid A, isochlorogenic acid B, and isochlorogenic acid C were separately prepared by accurately weighing appropriate amounts of

reference compounds into separate flasks. In the flasks, blank plasma was added, and the solutions were diluted with methanol to remove protein and miscible. An appropriate volume of the above nine individual stock solutions was mixed and diluted with methanol to generate the first working solution, which contained 0.97 ng/mL rutin, 10.04 ng/mL caffeic acid, 30.00 ng/mL chlorogenic acid, 16.40 ng/mL cryptochlorogenic acid, 20.00 ng/mL dispsacoside B, 18.28 ng/mL macranthoidin B, 21.20 ng/mL isochlorogenic acid A, 20.02 ng/mL isochlorogenic acid B, and 23.44 ng/mL isochlorogenic acid C. Subsequently, a dilution series of different concentrations of the mixed solutions were prepared to generate the corresponding regression data of the nine anti-inflammatory components. The QC samples were prepared at concentrations of 19.40 ng/mL for rutin, 1 004.00 ng/mL for caffeic acid, 15 000.00 ng/mL for chlorogenic acid, 1 640.00 ng/mL for cryptochlorogenic acid, 2 000.00 ng/mL for dispsacoside B, 1 828.00 ng/mL for macranthoidin B, 1 060.00 ng/mL for isochlorogenic acid A, 500.50 ng/mL for isochlorogenic acid B, and 2 344.00 ng/mL for isochlorogenic acid C. All solutions were stored at 4 °C before use.

2.8 Method validation

2.8.1 Specificity Specificity was evaluated by comparing different chromatograms of blank plasma samples spiked with the nine chemical standards, and plasma samples obtained from mice after oral administration of LJF or LF solutions.

2.8.2 Linearity and slower limit of quantification (LLOQ)

The calibration curves were determined by plotting the peak area (Y) and the plasma concentrations (X) of the nine anti-inflammatory components. LLOQ of the assay on the calibration curve was evaluated on the basis of a Signal/Noise (S/N) ratio of 10 : 1.

2.8.3 Precision The precision of the UPLC-QTOF-MS/MS method was confirmed by determining the nine anti-inflammatory components in the mixed standard solutions of the same brand. To evaluate the intra-day precision, the mixed standard solutions of the same brand were tested repeatedly for six times on the same day. This process continued for three consecutive days to determine the inter-day precision. Then calibration curves above were employed to determine the nine anti-inflammatory components in these tested samples. Acceptable criteria of the precision should be less than 15% for PK analysis.

2.8.4 Stability Stabilities of the nine anti-inflammatory components in mice plasma were evaluated by analyzing the mixed standard solutions of the same brand at 0.08, 0.25, 0.50, 0.75, 1.00, 2.00, 4.00, 6.00, and 8.00 h, respectively.

2.8.5 Extraction recovery Extraction recoveries of the nine anti-inflammatory components were investigated

using the mixed standard solutions of the same brand by calculating the mean peak area of the components in the extracted plasma samples to the area of post-extracted samples spiked with the target components at the same concentration level.

2.9 Data analysis

The compartmental model analysis was fitted by SPSS 21.0 software, and the classical PK parameters were calculated with Drug And Statistics (DAS) 2.1.1 software. The TQSM parameters were calculated with home-brew programs with Excel software. The TQSMS was obtained by converting TQSM parameters to NDPDF with Excel software. The measurement data were expressed as mean \pm standard deviation (SD). Independent-sample *t* test or non-parametric test was performed by SPSS 21.0 software to compare the differences of PK parameters and TQSM parameters. $P < 0.05$ was considered statistically significant.

3 Results

3.1 UPLC-QTOF-MS/MS method validation

3.1.1 Specificity Representative MRM chromatograms obtained from blank plasma samples spiked with nine chemical standards, and the plasma samples after oral administration of LJF or LF solutions were shown in Figure 3. Although the same precursor/production ions (609.1/300.0) were obtained for isochlorogenic acid A, isochlorogenic acid B, and isochlorogenic acid C, their chromatograms could achieve base separation due to polarity difference. No significant endogenous components were observed to interfere with the analysis of the nine anti-inflammatory components.

3.1.2 Linearity and LLOQ Linear regression equations for calibration curves of the nine anti-inflammatory components within the tested ranges were summarized in Table 2. And the correlation coefficients of all components were fluctuated from 0.999 1 to 0.999 9 in the linear range. It was also observed that LLOQs of the nine anti-inflammatory components ranged from 0.49 to 91.40 ng/mL. The above results suggested that the proposed method was sensitive enough to determine the nine anti-inflammatory components in plasma samples.

3.1.3 Precision The precision variations (RSD) of these nine anti-inflammatory components were from 0.89% to 5.72%. All the assay values met the acceptable criteria (15%), and hence indicating favorable data for precision of this developed UPLC-QTOF-MS/MS method.

3.1.4 Stability The stability of the nine anti-inflammatory components of assayed samples was tested under analysis conditions to obtain the RSD of 0.33% to 4.02%. All compounds were shown to be stable in plasma samples within 24 h.

3.1.5 Extraction recovery The average recovery of each component was 95.0% to 105.0%, suggesting that the recovery rate met the requirements. These data indicated that this analytical method could meet the requirement of the assays.

3.2 Conventional comparisons by single-component PK parameters

The mean plasma concentration-time curves of the nine anti-inflammatory components after oral administration of LJF and LF in mice with acute inflammation were illustrated in Figure 4. The PK profiles of the three components (caffeic acid, dispsacoside B, and macranthoidin B) were better fitted to the one-compartment model, and the other six components (rutin, chlorogenic acid, cryptochlorogenic acid, isochlorogenic acid A, isochlorogenic acid B, and isochlorogenic acid C) to the two-compartment model through classical compartmental model analysis by DAS software.

The PK parameters of the nine anti-inflammatory components fitted to the one or two-compartment models were calculated and presented in Table 3 and Table 4, respectively. The main parameters, i.e. absorption rate constant (K_a), absorption half-life ($T_{1/2Ka}$), peak concentration (C_{max}), and peak time (T_{max}) of the nine components of LJF were as $(3.384\ 0 \pm 0.054\ 4) - (33.401\ 7 \pm 2.183\ 5)\ h^{-1}$, $(0.020\ 8 \pm 0.001\ 4) - (0.229\ 9 \pm 0.084\ 4)\ h$, $(0.272\ 3 \pm 0.004\ 9) - (16.795\ 3 \pm 0.410\ 3)\ \mu\text{g/mL}$, and $(0.331\ 1 \pm 0.002\ 3) - (0.681\ 1 \pm 0.128\ 6)\ h$, respectively. Whereas those of LF were $(2.526\ 0 \pm 0.006\ 1) - (10.727\ 8 \pm 0.557\ 7)\ h^{-1}$, $(0.064\ 7 \pm 0.003\ 3) - (0.274\ 3 \pm 0.000\ 7)\ h$, $(0.011\ 1 \pm 0.000\ 2) - (25.409\ 8 \pm 0.734\ 5)\ \mu\text{g/mL}$, and $(0.317\ 3 \pm 0.000\ 7) - (0.423\ 4 \pm 0.000\ 7)\ h$, respectively. The *P* values of the PK parameters of all the single components varied from 0.000 0 to 0.870 1, showing partial significant differences and similarities of PK profiles.

3.3 Integral comparison among TQSM parameters of single component and multiple components

Based on SM properties, PK profiles were converted into PPK profiles to obtain the TQSM parameters (Table 5). The TQSM parameters (AUC_{T_0-t} , $AUC_{T_0-\infty}$, MRT_{T_0-t} , $MRT_{T_0-\infty}$, and $VRT_{T_0-\infty}$) for the quanta of the nine components in LJF were $(51.330\ 1 \pm 1.221\ 9)\ \mu\text{g}\cdot\text{h/mL}$, $(56.429\ 4 \pm 1.774\ 7)\ \mu\text{g}\cdot\text{h/mL}$, $(2.037\ 5 \pm 0.034\ 5)\ h$, $(3.908\ 2 \pm 0.117\ 6)\ h$, and $(9.069\ 0 \pm 1.256\ 7)\ h^2$, respectively; whereas those in LF were $(58.429\ 3 \pm 6.947\ 3)\ \mu\text{g}\cdot\text{h/mL}$, $(67.151\ 9 \pm 10.814\ 4)\ \mu\text{g}\cdot\text{h/mL}$, $(1.726\ 0 \pm 0.300\ 0)\ h$, $(3.434\ 6 \pm 0.293\ 8)\ h$, and $(15.246\ 6 \pm 5.479\ 2)\ h^2$, respectively. The *t* test or non-parametric test was performed to compare the differences in PK parameters of LJF and LF. Although there were great differences in TQSM parameters of single component ($P < 0.05$), no significant differences were found in the TQSM parameters for the quanta of the nine anti-inflammatory components ($P > 0.05$).

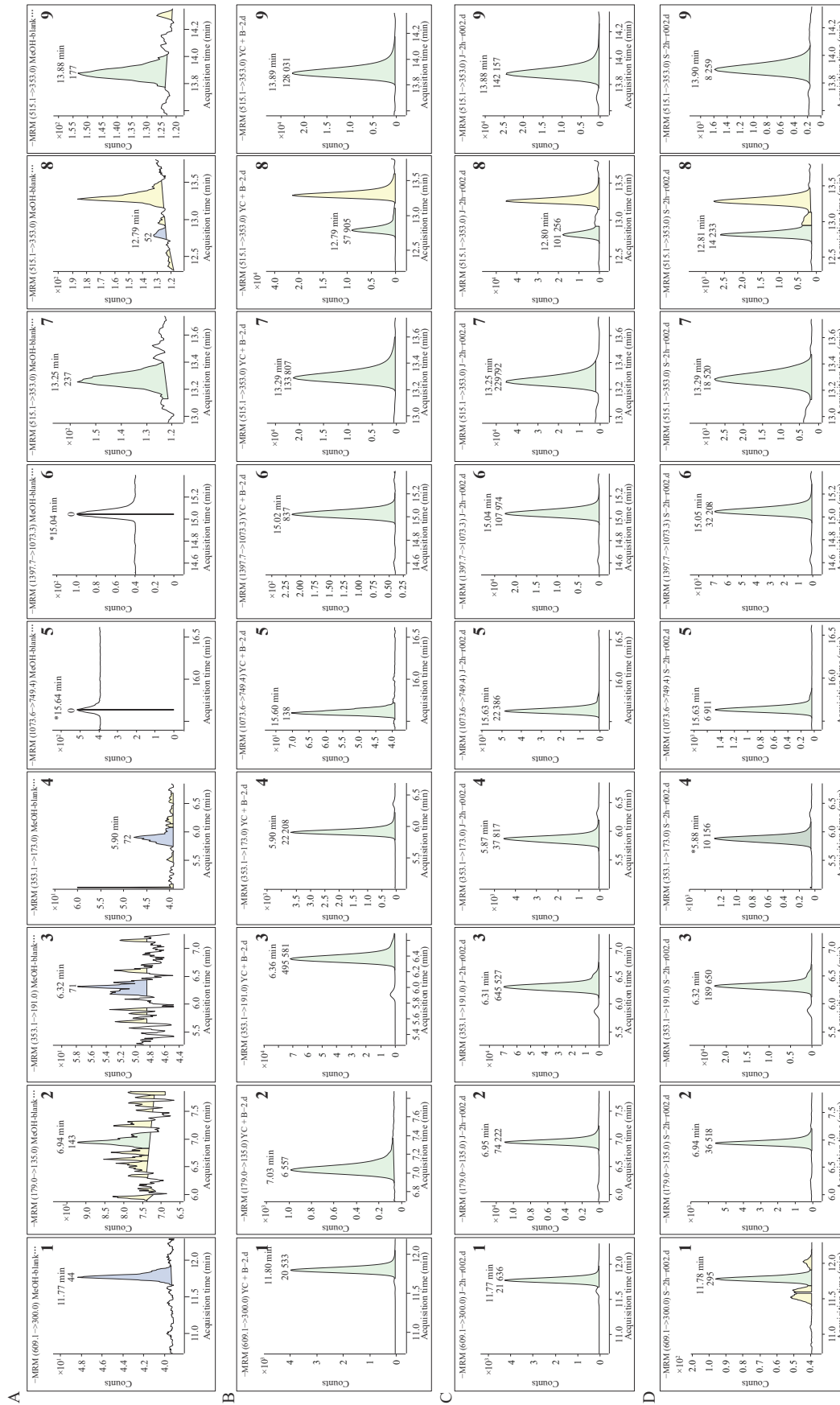
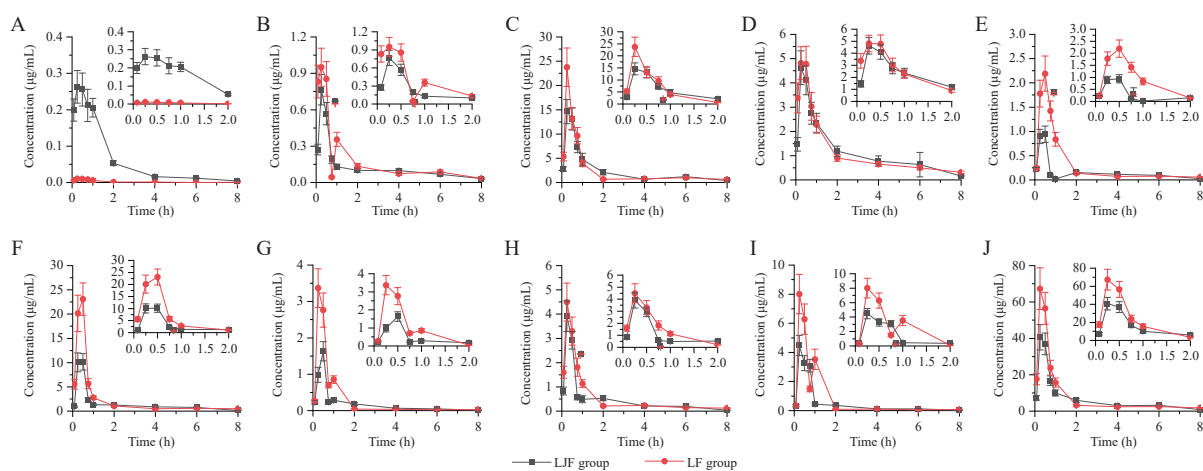


Figure 3 Representative MRM chromatograms of the nine anti-inflammatory components in four different types of plasma samples

A, blank plasma samples. B, blank plasma samples spiked with nine chemical standards. C, plasma samples collected at 2 h following oral administration of LJF extract. D, plasma samples collected at 2 h following oral administration of LF extract. 1 represents rutin. 2 represents caffeic acid. 3 represents chlorogenic acid. 4 represents isochlorogenic acid. 5 represents dispsacoside B. 6 represents macranthoidin B. 7 represents isochlorogenic acid A. 8 represents isochlorogenic acid B. 9 represents isochlorogenic acid C.

Table 2 Linear regression data of the nine anti-inflammatory components in LJF and LF

No.	Component	Range (ng/mL)	Linear regression equation	Correlation coefficient	LLOQ (ng/mL)
1	Rutin	0.49 – 970.00	$Y = 43.23X + 110.53$	0.999 4	0.49
2	Caffeic acid	50.20 – 10 040.00	$Y = 70.93X + 1 260.60$	0.999 8	50.20
3	Chlorogenic acid	3.00 – 30 000.00	$Y = 26.86X + 2 152$	0.999 1	3.00
4	Cryptochlorogenic acid	8.20 – 16 400.00	$Y = 3.14X + 184.74$	0.999 5	8.20
5	Dispsacoside B	10.00 – 20 000.00	$Y = 16.20X - 1 069.40$	0.999 7	10.00
6	Macranthoidin B	91.40 – 18 280.00	$Y = 8.56X - 566.67$	0.999 9	91.40
7	Isochlorogenic acid A	10.60 – 21 200.00	$Y = 124.64X + 3 508.10$	0.999 5	10.60
8	Isochlorogenic acid B	20.02 – 20 020.00	$Y = 18.15X + 976.54$	0.999 8	20.02
9	Isochlorogenic acid C	11.72 – 23 440.00	$Y = 41.01X - 3 434$	0.999 8	11.72

**Figure 4** Mean plasma concentration-time curves of the nine anti-inflammatory components in mice with acute inflammation after oral administration of LJF and LF (mean \pm SD, $n = 3$)

A, rutin. B, caffeic acid. C, chlorogenic acid. D, cryptochlorogenic acid. E, dispsacoside B. F, macranthoidin B. G, isochlorogenic acid A. H, isochlorogenic acid B. I, isochlorogenic acid C. J, total quanta of the nine anti-inflammatory components.

3.4 TQSMS of single component and multiple components

TQSM parameters (AUC_T , MRT_T , and VRT_T) were investigated to present integral PPK profiles of the nine anti-inflammatory components. Furthermore, to compare the similarity or difference straightforwardly, MRT_T and VRT_T of the nine anti-inflammatory components, as mean and variance, were then integrated with the NDPDF to yield overlapped areas, which was defined to TQSMS. Moreover, TQSMS of single and multiple components were calculated (Figure 5). Although the TQSMS of a single component fluctuated from 0.220 4 to 0.968 9, the TQSMS of the total quanta was 0.828 4. Interestingly, the similarity of chlorogenic acid (0.924 1) was the largest among all the TQSMS, which is the most critical quality marker for both LJF and LF in the *Chinese Pharmacopoeia*.

Furthermore, the total concentrations and TQSM parameters (MRT_{T0-t} and VRT_{T0-t}) of the components at different time points were calculated and compared (Table 6). No significant differences were found in the total contents and MRT_{T0-t} of the total quanta ($P > 0.05$).

4 Discussion

The results demonstrated significant differences only in part of the single-component PK parameters (Table 3 and 4). For instance, significant differences were found in the C_{max} of rutin, while no significant difference in that of cryptochlorogenic acid. Besides, the PPK profile's similarity or difference is difficult to be thoroughly evaluated by single-component PK parameters. Consequently, the PPK model and its TQSMS method were carried out to compare the integral similarity or difference of LJF and LF comprehensively.

As depicted in Table 5, there were no significant differences in TQSM parameters (AUC_{T0-t} , $AUC_{T0-\infty}$, MRT_{T0-t} , $MRT_{T0-\infty}$, and $VRT_{T0-\infty}$) of the total quanta of the nine anti-inflammatory components of LJF and LF, which indicated that the extent and speed of bioavailability had no significant differences, either. The results were consistent with previous literature that the AUC_T , MRT_T , and VRT_T of the entire chromatographical fingerprints of LJF and LF had no significant differences [23]. As revealed by the above results, the PPK model could be an appropriate

Table 3 PK parameters of the three anti-inflammatory components fitted to the one-compartment model after oral administration of LJF or LF

Component	Group	K_a (h ⁻¹)	K (h ⁻¹)	$T_{1/2 K_a}$ (h)	$T_{1/2 K}$ (h)	C_{max} (ug/mL)	T_{max} (h)
Caffeic acid	LJF	3.915 0 ± 0.020 8	3.713 3 ± 0.020 8	0.177 0 ± 0.000 8	0.186 6 ± 0.001 0	0.823 7 ± 0.003 0	0.331 1 ± 0.002 3
	LF	8.903 7 ± 0.268 7***	2.538 7 ± 0.052 2***	0.077 9 ± 0.002 4***	0.273 1 ± 0.005 6***	1.414 3 ± 0.798 5	0.337 8 ± 0.065 9
Dispasoside B	LJF	3.770 0 ± 0.071 4	3.745 3 ± 0.117 4	0.183 9 ± 0.003 5	0.185 2 ± 0.005 8	1.063 7 ± 0.014 5	0.385 0 ± 0.005 7
	LF	2.526 0 ± 0.006 1***	2.358 7 ± 0.010 7***	0.274 3 ± 0.000 7***	0.293 8 ± 0.001 3***	9.538 0 ± 12.550 5	0.423 4 ± 0.000 7***
Macranthoidin B	LJF	3.384 0 ± 0.054 4	3.225 3 ± 0.044 4	0.204 8 ± 0.003 3	0.214 9 ± 0.003 0	12.139 9 ± 0.389 4	0.377 0 ± 0.005 9
	LF	3.488 0 ± 0.063 2	3.336 0 ± 0.061 1	0.198 7 ± 0.003 6	0.207 8 ± 0.003 8	24.793 5 ± 0.796 3***	0.396 3 ± 0.019 5

Values are expressed as mean ± SD (n = 3). ***P < 0.001, compared with the LJF group. K_a represents absorption rate constant. K represents eliminating speed constants. $T_{1/2 K_a}$ represents absorption half-life. $T_{1/2 K}$ represents eliminating half-life. C_{max} represents maximum concentration. T_{max} represents peak time.

Table 4 PK parameters of the six anti-inflammatory components fitted to the two-compartment model after oral administration of LJF or LF

Component	Group	K_a (h ⁻¹)	α (h ⁻¹)	β (h ⁻¹)	$T_{1/2 K_a}$ (h)	$T_{1/2 \alpha}$ (h)	$T_{1/2 \beta}$ (h)	C_{max} (ug/mL)	T_{max} (h)
Rutin	LJF	4.108 7 ± 0.683 1	1.134 3 ± 0.012 7	5.188 3 ± 1.407 1	0.229 9 ± 0.084 4	0.661 8 ± 0.004 9	0.188 8 ± 0.021 4	0.272 3 ± 0.004 9	0.365 9 ± 0.015 1
	LF	5.323 7 ± 2.228 8	2.126 7 ± 1.935 4	0.129 7 ± 0.000 7*	0.136 7 ± 0.116 9	0.221 7 ± 0.044 5	1.786 1 ± 0.011 1*	0.011 1 ± 0.000 2***	0.359 6 ± 0.011 2
Chlorogenic acid	LJF	5.001 0 ± 0.513 4	3.920 3 ± 0.153 9	0.198 0 ± 0.112 1	0.139 6 ± 0.014 8	0.177 0 ± 0.007 1	5.070 8 ± 4.185 7	16.795 3 ± 0.410 3	0.358 3 ± 0.004 3
	LF	10.727 8 ± 0.557 7***	3.275 6 ± 0.035 0**	0.158 6 ± 0.000 4	0.064 7 ± 0.003 3**	0.211 6 ± 0.002 3**	4.370 6 ± 0.012 3	25.409 8 ± 0.734 5***	0.317 3 ± 0.000 7***
Cryptochlorogenic acid	LJF	33.401 7 ± 2.183 5	21.619 0 ± 0.914 6	1.992 7 ± 0.020 0	0.020 8 ± 0.001 4	0.032 1 ± 0.001 4	0.347 8 ± 0.003 5	5.174 1 ± 0.164 5	0.354 2 ± 0.002 5
	LF	3.500 7 ± 0.241 5***	3.181 3 ± 0.317 0***	0.124 3 ± 0.013 4***	0.198 6 ± 0.013 7***	0.219 3 ± 0.021 9***	5.620 1 ± 0.643 8***	5.122 0 ± 0.193 2	0.372 8 ± 0.010 8*
Isochlorogenic acid A	LJF	6.364 7 ± 3.870 3	9.939 7 ± 10.668 1	5.212 3 ± 2.486 1	0.133 2 ± 0.060 0	0.132 6 ± 0.087 9	0.150 9 ± 0.056 4	1.789 3 ± 0.167 0	0.681 1 ± 0.128 6
	LF	5.959 0 ± 0.853 7	4.989 3 ± 0.949 9	79.577 3 ± 18.111 1	0.117 8 ± 0.015 6	0.142 0 ± 0.024 5	0.015 5 ± 0.012 2*	3.881 4 ± 0.061 4***	0.351 0 ± 0.002 4*
Isochlorogenic acid B	LJF	7.579 3 ± 1.450 9	4.405 7 ± 0.400 0	37.000 7 ± 19.022 4	0.093 9 ± 0.019 4	0.158 1 ± 0.013 7	0.021 7 ± 0.008 7	4.332 6 ± 0.073 0	0.338 1 ± 0.006 2
	LF	7.987 5 ± 4.693 4	2.779 0 ± 1.608 8*	0.078 0 ± 0.044 6	0.087 8 ± 0.051 6	0.249 8 ± 0.144 6**	9.100 0 ± 5.437 2**	4.832 3 ± 0.148 5**	0.330 1 ± 0.004 1
Isochlorogenic acid C	LJF	5.299 7 ± 0.700 6	4.490 7 ± 1.401 0	1.017 3 ± 1.540 4	0.132 2 ± 0.016 2	0.163 3 ± 0.043 2	3.692 2 ± 2.983 2	5.066 0 ± 0.074 5	0.340 9 ± 0.000 3
	LF	7.138 0 ± 0.204 5*	5.867 3 ± 0.457 6	1.169 7 ± 0.017 0	0.097 1 ± 0.002 8*	0.118 6 ± 0.009 4	0.592 6 ± 0.008 6	9.129 2 ± 0.100 3***	0.348 9 ± 0.002 1**

Values are expressed as mean ± SD (n = 3). *P < 0.05, **P < 0.01, and ***P < 0.001, compared with the LJF group. K_a represents absorption rate constant. $T_{1/2 K_a}$ represents absorption half-life. α represents distributed speed constant. $T_{1/2 \alpha}$ represents distribution half-life. β represents eliminating speed constants. $T_{1/2 \beta}$ represents eliminating half-life. C_{max} represents maximum concentration. T_{max} represents peak time.

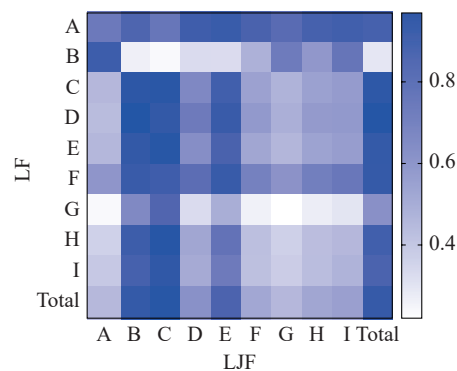
Table 5 TQSM parameters of single component and the quanta of the nine anti-inflammatory components after oral administration of LJF or LF

Component	Group	AUC_{0-t} (ug·h/mL)	$AUC_{0-\infty}$ (ug·h/mL)	MRT_{0-t} (h)	$MRT_{0-\infty}$ (h)	$VRT_{0-\infty}$ (h ²)
Rutin	LJF	0.468 6 ± 0.033 9	0.474 0 ± 0.034 7	1.469 6 ± 0.017 2	1.636 0 ± 0.020 0	1.362 7 ± 0.051 3
	LF	0.013 2 ± 0.000 5 ^{***}	0.014 2 ± 0.000 6 ^{***}	1.661 5 ± 0.043 1*	2.282 7 ± 0.050 6**	4.878 7 ± 0.055 8 ^{***}
Caffeic acid	LJF	0.975 5 ± 0.014 2	1.157 1 ± 0.014 2	2.433 9 ± 0.004 4	4.187 4 ± 0.025 3	9.923 7 ± 0.082 7
	LF	1.304 7 ± 0.036 0 ^{***}	1.455 2 ± 0.036 0 ^{***}	2.070 1 ± 0.040 1 ^{***}	3.138 6 ± 0.010 1 ^{***}	7.112 2 ± 0.272 9 ^{***}
Chlorogenic acid	LJF	18.769 9 ± 1.602 6	22.522 4 ± 2.325 0	1.928 1 ± 0.092 1	4.422 9 ± 0.326 2	20.163 1 ± 1.020 5
	LF	18.851 8 ± 0.230 4	22.713 3 ± 0.241 3	1.693 1 ± 0.014 2*	3.810 5 ± 0.017 5*	15.124 2 ± 0.109 3**
Cryptochlorogenic acid	LJF	9.418 5 ± 0.572 6	9.946 9 ± 0.564 9	2.495 5 ± 0.247 1	2.962 0 ± 0.202 3	2.109 2 ± 0.711 9
	LF	8.767 9 ± 0.1005	10.497 9 ± 0.148 8	2.200 0 ± 0.050 0	4.062 8 ± 0.004 6 ^{***}	11.144 7 ± 0.157 8 ^{***}
Dispsacoside B	LJF	1.166 6 ± 0.037 2	1.288 3 ± 0.036 4	2.509 4 ± 0.019 1	3.462 0 ± 0.056 7	5.174 0 ± 0.245 3
	LF	2.379 5 ± 0.039 4 ^{***}	2.805 2 ± 0.034 9 ^{***}	1.461 6 ± 0.013 6 ^{***}	3.601 9 ± 0.059 4 ^{***}	17.441 7 ± 0.263 8 ^{***}
Macranthoidin B	LJF	11.653 9 ± 0.226 0	11.962 9 ± 0.224 6	2.105 3 ± 0.021 9	2.314 1 ± 0.026 2	1.435 5 ± 0.093 1
	LF	18.099 0 ± 0.599 2 ^{***}	20.347 8 ± 0.872 3 ^{***}	1.384 2 ± 0.057 8 ^{***}	2.632 3 ± 0.143 6 ^{***}	9.847 6 ± 0.556 1**
Isochlorogenic acid A	LJF	1.389 1 ± 0.113 6	1.412 2 ± 0.115 3	1.577 1 ± 0.186 2	1.718 8 ± 0.179 7	1.167 5 ± 0.074 6
	LF	2.359 4 ± 0.055 5 ^{***}	2.929 5 ± 0.048 7 ^{***}	0.911 6 ± 0.003 4**	5.894 3 ± 0.143 4 ^{***}	74.492 2 ± 1.459 8 ^{***}
Isochlorogenic acid B	LJF	3.750 2 ± 0.177 8	3.839 6 ± 0.189 7	1.843 6 ± 0.078 3	2.049 8 ± 0.095 1	1.565 8 ± 0.026 3
	LF	4.322 5 ± 0.032 9**	5.418 6 ± 0.142 8 ^{***}	1.603 8 ± 0.004 0**	4.735 8 ± 0.225 9 ^{***}	25.149 3 ± 1.099 6 ^{***}
Isochlorogenic acid C	LJF	3.901 7 ± 0.039 0	3.989 2 ± 0.039 1	1.354 9 ± 0.011 6	1.561 2 ± 0.018 4	2.008 5 ± 0.067 7
	LF	6.316 7 ± 0.059 1 ^{***}	7.219 6 ± 0.114 8 ^{***}	0.936 1 ± 0.008 7 ^{***}	3.436 5 ± 0.166 8 ^{***}	31.272 8 ± 1.692 3 ^{***}
Average	LJF	5.721 1 ± 6.057 3	6.288 1 ± 7.070 1	1.968 6 ± 0.439 6	2.701 6 ± 1.070 0	4.990 0 ± 6.123 8
	LF	6.935 0 ± 6.783 4	8.155 8 ± 7.909 0	1.551 2 ± 0.425 3	3.738 2 ± 1.048 2	21.833 8 ± 20.668 6

Values are expressed as mean ± SD ($n = 3$). * $P < 0.05$, ** $P < 0.01$, and *** $P < 0.001$, compared with the LJF group. AUC_{0-t} represents zero moment within time 0 to t . $AUC_{0-\infty}$ represents zero moment within time 0 to infinite. MRT_{0-t} represents first moment within time 0 to t . $MRT_{0-\infty}$ represents first moment within time 0 to infinite. $VRT_{0-\infty}$ represents second moment within time 0 to infinite.

tool to integrate single-component PK parameters into TQSM parameters, but could not evaluate the similarity or difference of PPK profiles directly.

Therefore, the TQSMS of single and multiple components was calculated based on these TQSM parameters to compare the similarity or difference of PK or PPK profiles, respectively. The TQSMS of single component ranged from 0.220 4 to 0.968 9, whereas 0.828 4 for the total quanta of the nine anti-inflammatory components (Figure 5). The results indicated the integral PPK profiles of LJF and LF are similar with almost the same anti-inflammatory efficacy, which is consistent with previous study [22]. Moreover, no significant difference was observed in the total concentrations of the nine anti-inflammatory components *in vivo* and MRT_{0-t} at different time points by t test, although their total concentration *in vitro* had significant differences (16 680.84 ug/mL for LJF and 60 002.48 ug/mL for LF, respectively) (Table 6). For example, the concentrations of organic acids in LF (chlorogenic acid, caffeic acid, isochlorogenic acid A, isochlorogenic acid B, and isochlorogenic acid C) is almost two to four times higher than those in LJF. The flavonoid (rutin)

**Figure 5** TQSMS of single component and all the nine anti-inflammatory components of LJF and LF

A represents rutin. B represents caffeic acid. C represents chlorogenic acid. D represents cryptochlorogenic acid. E represents dispsacoside B. F represents macranthoidin B. G represents isochlorogenic acid A. H represents isochlorogenic acid B. I represents isochlorogenic acid C. Total represents total quanta for the nine anti-inflammatory components. The different degrees of color clearly indicate the similarity size between the nine chemical components in LJF and LF (0.220 4 to 0.968 9). The darker the colors, the higher the similarity.

Table 6 TQSM parameters and total content of LJF and LF at different designed time points

Time (h)	LJF			LF		
	Total content (ug/mL)	MRT_{T0-t} (h)	VRT_{T0-t} (h ²)	Total content (ug/mL)	MRT_{T0-t} (h)	VRT_{T0-t} (h ²)
0.08	7.276 9 ± 0.111 4	9.112 0 ± 0.038 6	14.362 3 ± 0.022 4	17.552 5 ± 0.265 8	9.997 5 ± 0.007 8	17.422 8 ± 0.124 8
0.25	40.601 9 ± 0.428 6	10.363 6 ± 0.034 9	16.393 6 ± 0.049 2	67.221 3 ± 0.878 0	10.847 3 ± 0.037 4	16.585 4 ± 0.070 9
0.50	36.928 0 ± 0.417 4	10.470 8 ± 0.053 6	16.710 0 ± 0.072 7	56.472 5 ± 1.114 6	11.820 7 ± 0.074 0	15.583 7 ± 0.162 4
0.75	16.754 1 ± 0.226 0	9.295 9 ± 0.066 7	15.337 9 ± 0.138 0	23.824 3 ± 0.253 6	10.067 9 ± 0.035 9	17.510 0 ± 0.071 9
1.00	10.259 2 ± 0.944 6	10.043 4 ± 0.014 6	16.147 1 ± 0.049 5	15.632 9 ± 0.133 9	10.853 2 ± 0.196 0	16.055 9 ± 0.342 3
2.00	5.897 2 ± 0.137 7	9.626 0 ± 0.022 7	16.377 6 ± 0.041 9	3.241 4 ± 0.031 9	10.212 4 ± 0.037 2	18.605 9 ± 0.073 5
4.00	2.892 4 ± 0.137 5	9.655 1 ± 0.024 8	15.954 2 ± 0.043 7	2.429 6 ± 0.052 0	9.352 1 ± 0.103 9	16.394 9 ± 0.336 9
6.00	0.170 6 ± 0.044 3	9.774 8 ± 0.023 4	16.159 7 ± 0.044 6	2.453 5 ± 0.012 6	9.274 0 ± 0.111 9	16.696 6 ± 0.324 0
8.00	0.858 8 ± 0.049 0	8.629 1 ± 0.004 6	15.770 0 ± 0.003 3	1.732 3 ± 0.055 2	9.839 6 ± 0.137 9	17.503 3 ± 0.250 1
<i>P</i>				0.868	0.097	0.013*

Values are expressed as mean ± SD ($n=3$). * $P < 0.05$, compared with the LJF group. MRT_{T0-t} represents total quantum first moment within time 0 to t . VRT_{T0-t} represents total quantum second moment within time 0 to t .

is almost undetectable in LF but is abundant in LJF. Besides, triterpenoid saponins are also the components that contributed to the distinction between LJF and LF, which are undetectable in LJF but abundant in LF. These concentration differences *in vitro* are consistent with previous literature [6]. Taken together, regardless of the differences of *in vitro* component concentration, the nine anti-inflammatory components of LJF and LF in the blood of mice have similar levels. Generally, the components that were absorbed *in vivo*, rather than the *in vitro* ones, are key components in CMM that ultimately determine its clinical efficacy. The results have explained the inconsistency between components *in vitro* and the CMM's clinical efficacy. Although the *in vitro* component concentrations are different, they yield similar pharmacological efficacy. Overall, these results suggest that LJF and LF produce almost the same anti-inflammatory efficacy in clinical treatment due to their similar PPK profiles and similar *in vivo* component concentrations, which could provide reference for their clinical use and reasonable record in *Chinese Pharmacopoeia*. LJF and LF had not been distinguished until the *Chinese Pharmacopoeia* (edition 2005) was published, which said they had same nature and flavour, meridian tropism, directions, and dosage. In addition to the concentration of components in the blood, the targets and the pathway also affect the similarity in their PPK profiles and pharmacological efficacy. Previous literature reported that LJF and LF shared 66.7% common targets and both blocked inflammation by nuclear factor kappa-B (NF- κ B) signalling pathway [24].

This study freshly applied the PPK model and its TQSMS method to compare the similarity or difference of PPK profiles of two CMMs, which bridges over chemical composition to their pharmacological efficacy. The

proposed method can be extensively applied to distinguish an increasing number of CMMs, especially those that are easily mixed up. However, this research still has its limitations. For instance, we only selected nine anti-inflammatory components and one of the four plant sources of LF for PPK study. The similarity or difference of integral PPK profiles should be compared more comprehensively by investigating more components in LJF and LF in the future. In addition, different plant sources of LF should also be investigated because there may be differences in experimental results for LF originated from different plant sources.

5 Conclusion

Unlike the previous PK study of single component which takes AUC , C_{max} and T_{max} as the main evaluation indexes, TQSM parameters and TQSMS were employed in this study to evaluate the integral PPK profiles' similarity or difference of the nine anti-inflammatory components of LJF and LF in p-xylene-induced ear edema mice. Despite the significant differences in PK parameters of single component and the total quanta of the nine components *in vitro*, there were no significant differences in the integral TQSM parameters of the total quanta and the total concentration of the nine components *in vivo*. Besides, the TQSMS was high due to the similarity of 0.828 4, indicating that the integral PPK profiles of the nine anti-inflammatory components of LJF and LF were similar. The PPK model and its TQSMS method could be a feasible and appropriate combination to integrate and evaluate multi-component PPK profiles.

All these findings have explained why different concentrations of the nine anti-inflammatory components of

LJF and LF *in vitro* have the same anti-inflammatory efficacy, suggesting the interchangeable use of LJF and LF for anti-inflammatory treatment in clinic.

Fundings

National Natural Science Foundation of China (81703824), Natural Science Foundation of Hunan Province (2021JJ80058 and 2021JJ30509), Research Fund and Joint Fund Project of Hunan University of Chinese Medicine (2021XJJ002), Postgraduate Teaching Platform Project of Hunan Province (Xiang Jiao Tong [2019] No. 334), and Postgraduate Research Innovation Program of Hunan Province (CX20210689).

Competing interests

The authors declare no conflict of interest.

References

- [1] ZHANG F, SHI PL, LIU HY, et al. A simple, rapid, and practical method for distinguishing *Lonicerae Japonicae* Flos from *Lonicerae Flos*. *Molecules*, 2019, 24(19): 3455.
- [2] ZHAO J, CUI P, LIU H, et al. Rapid screening and quantitative analysis of adulterant *Lonicerae Flos* in *Lonicerae Japonicae Flos* by Fourier-transform near infrared spectroscopy. *Infrared Physics & Technology*, 2019, 104: 103139.
- [3] WANG Z, WEN HL, MEI SM. Discussion on the variety classification of *Lonicerae Japonicae Flos* and *Lonicerae Flos* in 2005 edition of *Chinese Pharmacopoeia*. *Lishizhen Medicine and Materia Medica Research*, 2009, 20(1): 150–151.
- [4] LI Y, LI W, FU C, et al. *Lonicerae Japonicae Flos* and *Lonicerae Flos*: a systematic review of ethnopharmacology, phytochemistry and pharmacology. *Phytochemistry Reviews*, 2020, 19(1): 1–61.
- [5] ZENG AQ, HUA H, CHEN CR, et al. Comparative study on anti-inflammatory effect of *Lonicerae Japonicae Flos* and *Lonicerae Flos*. *China Journal of Chinese Materia Medica*, 2020, 45(16): 3938–3944.
- [6] LIU RY, DENG J, LIIN XL, et al. Metabolomics reveals distinct metabolites between *Lonicera japonica* and *Lonicera macranthoides* based on GC-MS. *Journal of Chemistry*, 2020, 2020: 6738571.
- [7] ZHOU Y, ZHOU T, PEI Q, et al. Pharmacokinetics and tissue distribution study of chlorogenic acid from *Lonicerae Japonicae Flos* following oral administrations in rats. *Evidence-Based Complementary and Alternative Medicine*, 2014, 2014: 979414.
- [8] ZHOU W, SHAN JJ, WANG SQ, et al. Simultaneous determination of caffeic acid derivatives by UPLC-MS/MS in rat plasma and its application in pharmacokinetic study after oral administration of *Flos Loniceræ-Fructus Forsythiæ* herb combination. *Journal of Chromatography B*, 2014, 949: 7–15.
- [9] LIN Z, GEHRI R, MOCHEL JP, et al. Mathematical modeling and simulation in animal health - Part II: principles, methods, applications, and value of physiologically based PK modelling in veterinary medicine and food safety assessment. *Journal of Veterinary Pharmacology and Therapeutics*, 2016, 39: 421–438.
- [10] LIU CX, CHENG YY, GUO DA, et al. A new concept on quality marker for quality assessment and process control of Chinese medicines. *Chinese Herbal Medicines*, 2017, 9(3): 3–13.
- [11] WANG P, LI K, TAO Y, et al. A novel strategy for poly-pharmacokinetics prediction of traditional Chinese medicine based on single constituent pharmacokinetics, structural similarity, and mathematical modeling. *Journal of Ethnopharmacology*, 2019, 236: 277–287.
- [12] LIU L, WANG S, XU QX, et al. Poly-pharmacokinetic strategy represented the synergy effects of bioactive compounds in a traditional Chinese medicine formula, *Sishen Wan* and its separated recipes to normal and colitis rats. *Journal of Separation Science*, 2021, 44(10): 2065–2077.
- [13] HE FY, LUO JY, DENG KW, et al. A study of total amount statistic moment for TCM pharmacokinetics. *World Science and Technology/Modernization of Traditional Chinese Medicine and Materia Medica*, 2006, 8(6): 13–18.
- [14] ZHANG YT, XIAO MF, LIAO Q, et al. Application of TQSM polypharmacokinetics and its similarity approach to ascertain Q-marker by analyses of transitivity *in vivo* of five candidates in Buyang Huanwu Injection. *Phytomedicine*, 2018, 45: 18–25.
- [15] FAN QM, LIU WL, YANG YT, et al. A new similarity method for assessment of pharmacokinetic interaction between flucloxacillin and midazolam. *Die Pharmazie*, 2019, 74: 397–405.
- [16] ZHOU J, FAN Q, ZHANG Y, et al. Novel mathematical model for the assessment of similarity of chromatographic fingerprints of volatile oil from *Houttuynia cordata*. *Pharmacognosy Magazine*, 2021, 17(73): 154–162.
- [17] GUO XY, YU X, ZHENG BQ, et al. Network pharmacology-based identification of potential targets of *Lonicerae Japonicae Flos* acting on anti-inflammatory effects. *BioMed Research International*, 2021, 2021: 5507003.
- [18] LI YJ, CAI WY, WENG XG, et al. *Lonicerae Japonicae Flos* and *Lonicerae Flos*: a systematic pharmacology review. *Evidence-Based Complementary and Alternative Medicine*, 2015, 2015: 905063.
- [19] SONG YL, WANG HM, NI FY, et al. Study on anti-inflammatory activities of phenolic acids from *Lonicerae Japonicae Flos*. *Chinese Traditional and Herbal Drugs*, 2015, 46(4): 490–495.
- [20] TANG YL, YIN L, ZHANG YD, et al. Study on anti-inflammatory therapeutic efficacy and correlative ingredients with pharmacodynamics detected in acute inflammation rat model serum from *Caulis Loniceræ Japonicae*. *Phytomedicine*, 2016, 23: 597–610.
- [21] YAMAOKA K. Statistical moments in pharmacokinetics. *Journal of Pharmacokinetics & Biopharmaceutics*, 1978, 6(6): 547–558.
- [22] DUNN A. Statistical moments in pharmacokinetics: models and assumptions. *Journal of Pharmacy and Pharmacology*, 1993, 45(10): 871–875.
- [23] HE H, YANG J, HU C, et al. Bioequivalency research between *Lonicerae Japonicae Flos* and *Lonicerae Flos* based on chromatokinetics. *Chinese Journal of Experimental Traditional Medical Formulae*, 2016, 22(16): 1–5.
- [24] GAO Y, WANG FX, LIU Q, et al. Comparison of anti-inflammatory effects of *Lonicerae Japonicae Flos* and *Lonicerae Flos* based on network pharmacology. *Chinese Herbal Medicines*, 2021, 13(3): 332–341.

金银花和山银花 9 种抗炎成分对二甲苯耳肿胀模型小鼠体内的多成分药代动力学比较研究

李海英^{a, bt}, 肖美凤^{a, b, ct}, 潘雪^{a, b, c}, 李文姣^{a, b}, 周逸群^{a, b, c}, 刘文龙^{a, b, c}, 贺福元^{a, b, c*}

a. 湖南中医药大学药学院, 湖南长沙 410208, 中国

b. 中药成药性与制剂制备湖南省重点实验室, 湖南长沙 410208, 中国

c. 湖南中医药大学中医药超分子机理与数理特征化实验室, 湖南长沙 410208, 中国

【摘要】目的 比较金银花(LJF)和山银花(LF)体内整体多成分药代动力学(PPK)相似性或差异性,为临床用药提供参考。**方法** 运用 PPK 模型及其总量统计矩相似性(TQSMS)方法比较 LJF 和 LF 中具有抗炎作用的 9 种成分(芦丁、咖啡酸、绿原酸、隐绿原酸、川续断皂苷乙、灰毡毛忍冬皂苷乙、异绿原酸 A、异绿原酸 B 和异绿原酸 C)整体 PPK 特征。54 只无特定病原体级(SPF)昆明(KM)小鼠分为 2 组($n=27$),每组根据不同测试时间点分为 9 个亚组($n=3$)。随后口服给予 LJF 或 LF 并复制对二甲苯耳肿胀模型小鼠。通过超高效液相色谱/四极杆飞行时间质谱(UPLC-QTOF-MS/MS)测定血浆中 9 种成分浓度。由药物与统计(DAS)软件分析获得单成分药代动力学(PK)参数,并由自编 Excel 程序分析获得多成分整体 PPK 参数[总量统计矩(TQSM)参数和 TQSMS]。**结果** LJF 与 LF 单成分 PK 参数存在显著差异($P < 0.05$),而多成分 TQSM 参数无显著差异,包括总量零阶矩(AUC_{T0-t} , $AUC_{T0-\infty}$)和总量一阶矩(MRT_{T0-t} , $MRT_{T0-\infty}$)($P > 0.05$)。相应地,单成分 TQSMS 为 0.220 4 - 0.968 9,而 9 种成分整体 TQSMS 为 0.828 4,表明 LJF 和 LF 生物利用的速度和程度没有显著差异。此外, TQSMS (0.828 4)较大,表明 LJF 和 LF 9 种抗炎成分整体 PPK 特征在 90% 置信区间下相似。**结论** PPK 模型及其 TQSMS 方法可能是比较多成分中药整体 PPK 相似性或差异性的一种合适且有效方法。本研究表明金银花和山银花临床治疗炎症时可替代使用。

【关键词】 金银花; 山银花; 多成分药代动力学模型; 总量统计矩相似度; 抗炎作用; 一致性